Fully Functionalizable β,β'-BODIPY Dimer: Synthesis, Structure, and Photophysical Signatures

Ismael J. Arroyo-Córdoba, Rebeca Sola-Llano, Nerea Epelde-Elezcano, Iñigo López Arbeloa, Virginia Martínez-Martínez, and Eduardo Peña-Cabrera

https://doi.org/10.1021/acs.joc.8b01429

J. Org. Chem. 2018, 83, 10186–10196

A Fully Functionalizable β–β´-BODIPY Dimer. Synthesis, Structure, and Photophysical Signatures

Ismael J. Arroyo-Córdoba,[†‡] Rebeca Sola-Llano,[¥‡] Nerea Epelde-Elezcano,[¥] Iñigo López Arbeloa,[¥] Virginia Martínez-Martínez *,[¥] and Eduardo Peña-Cabrera.*,[†]

[†] Departamento de Química. Universidad de Guanajuato. Noria Alta S/N. Guanajuato, Gto. 36050. Mexico

[¥] Departamento de Química Física. Universidad del País Vasco-EHU, Apartado 644, 48080, Bilbao, Spain.

Email: virginia.martinez@ehu.eus, eduardop@ugto.mx

ABSTRACT: The versatility in the synthesis of BODIPY derivatives in terms of functionalization is further demonstrated. Particularly, in this work β–β'-BODIPY dimers with varied functional groups in the *meso*-positions were synthetized in a very efficient yields and short reaction times from a single platform. A photophysical study was carried in all the compounds. The resultant dimers show absorption bands at around 600 nm as a consequence of electronically coupled monomers disposed with a dihedral angle of around 30º, which is supported by theoretical simulations. The emission properties of these molecules are distinguished by the appearance of an ICT state as the polarity of the solvent increases.

Introduction

Reports on the reactivity, functionalization, applications, and structural studies of borondipyrromethenes (BODIPYs)[1] are far from being exhausted. Note that most of what has been developed deals with monomeric BODIPYs **1** and their fascinating properties (*i.e.*, large extinction coefficients, high quantum yields, excellent solubility in most organic solvents, resistant to photobleaching).[2–6] Additionally, they can be tailor-made by the functionalization of *each* their positions to fine-tune their properties for a desired application such as sensors (polarity, viscosity, pH), laser dyes, biotrackers, antenna systems, photosensitizers among others.[7–15]

One can only imagine the wealth of new applications that could arise from the structure and properties of two or more *directly linked* BODIPY fragments. In this sense, depending on the position of the union between BODIPY units and the nature of the substituents present in their structure, very different photophysical properties can be found. The systematic study of such compounds would lead to diverse and interesting applications in many research fields. However, there are only a few reports which describe some aspects of dimeric and oligomeric analogues (Figure 1).[16–24]

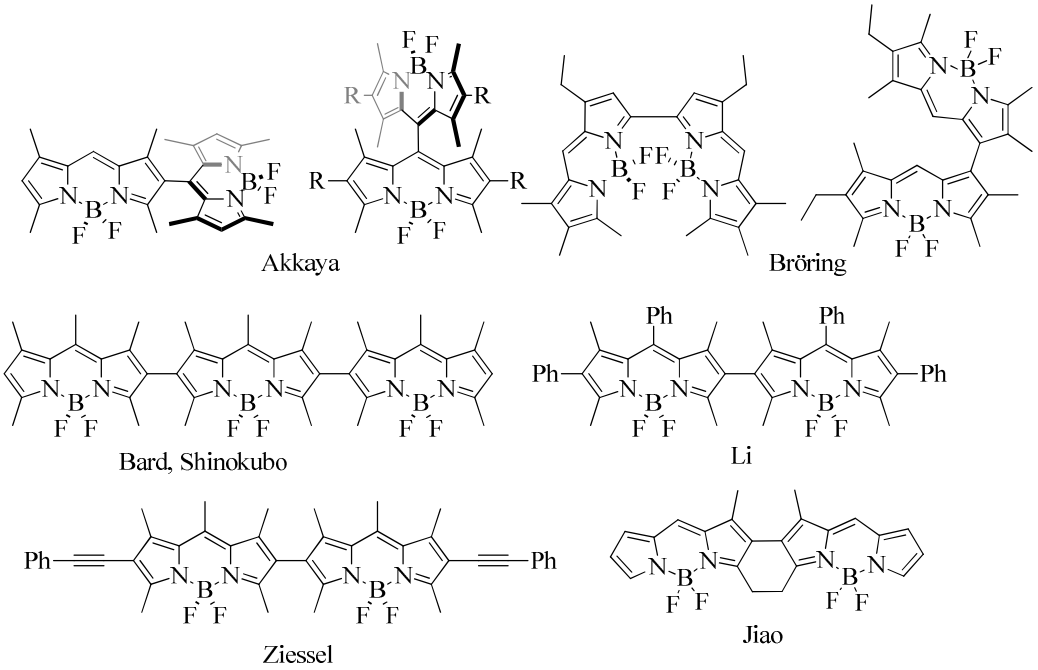

Figure 1. Examples of directly linked BODIPY dimers and trimers.

Nevertheless, their synthetic methodology is not suitable for a systematic, diversified and oriented functionalization. Indeed, to design BODIPY dimers for a specific application, one should be able to functionalize them at will.

The sought-after dimer **(**Figure 1**)** is thus endowed with several reaction sites that can be decorated with functional groups required for a particular application. A plethora of transformations can be envisioned, *i.e.*, chemoselective brominations,[21,25] formylations C-H activations,[26] Knoevenagel condensations,[27] modification of the B center with other heteroatoms or C-substituents,[28-30] together with the host of possibilities that the methylsulfanyl group offers (in turn, cross-couplings with either aryl boronic acids or organostannanes, desulfitative reduction, S_NAr-type reactions with phenols, alcohols, amines, thiols, stabilized *C*-centered nucleophiles).[12]

Herein, we disclose the synthesis and functionalization of a β,β´-BODIPY dimer (Figure 2), together with their main photophysical signatures.

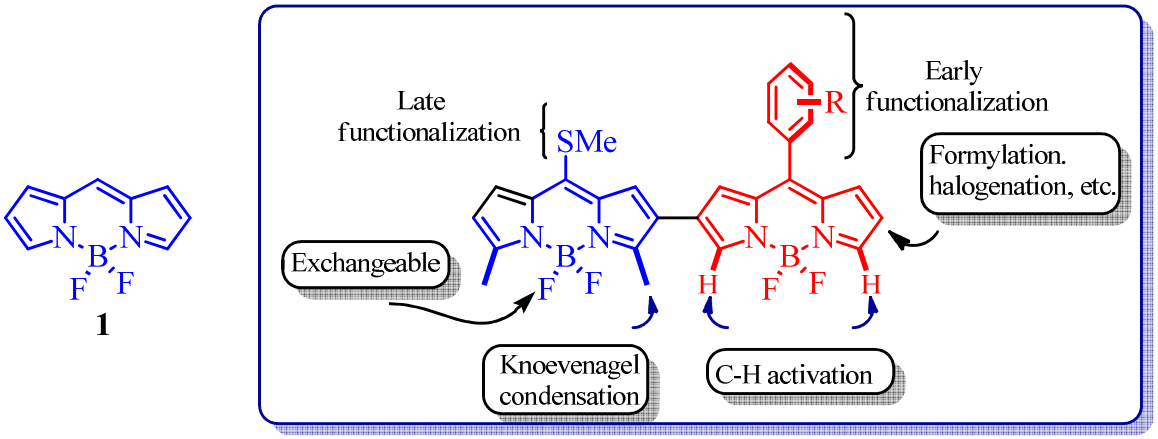

Figure 2. A fully functionalizable β,β´-BODIPY dimer.

Results and Discussion.

Synthesis. The dimer we chose to prepare, consists of two BODIPY units that can be functionalized at different stages. Mesityl-substituted BODIPY dimer **4** was prepared in good yield (80%) and short reaction time (Scheme 1).

Scheme 1. Synthesis of dimer **4.**

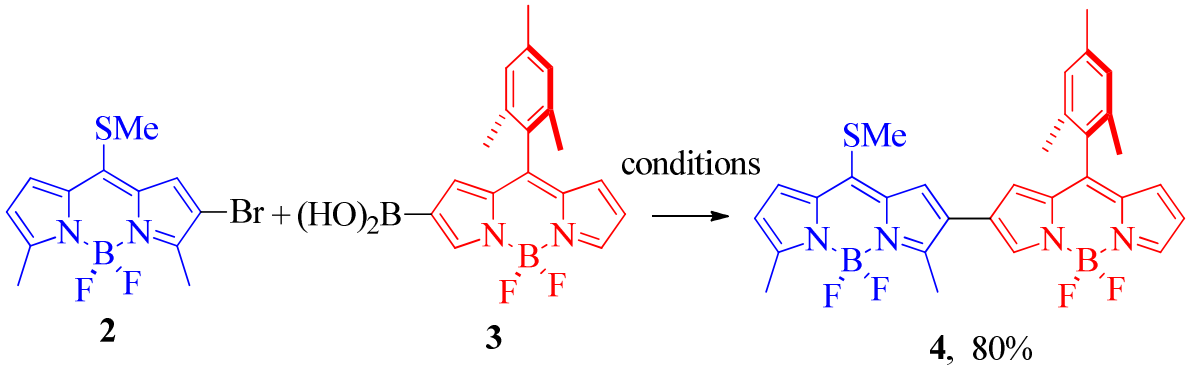

conditions: 5% $Pd(OAc)_2$, 12.5% S-Phos, 3.5 KOAc, toluene/H_2O (100:1)
90 °C, 20 min

BODIPY **2** was easily prepared from the NBS bromination of commercially available 2,6-dimethyl-8-methylthioBODIPY (eq. 1).

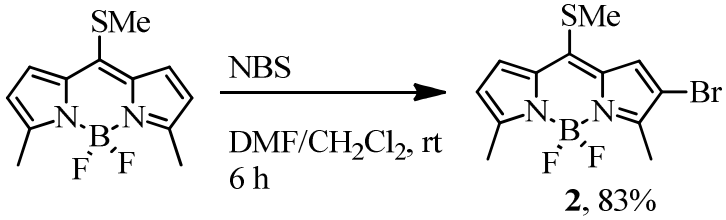

(1)

Boronic acid **3** was synthesized by deprotecting the corresponding pinacol boronic ester **A**,[31] previously reported by Shinokubo et al.[21] (eq. 2).

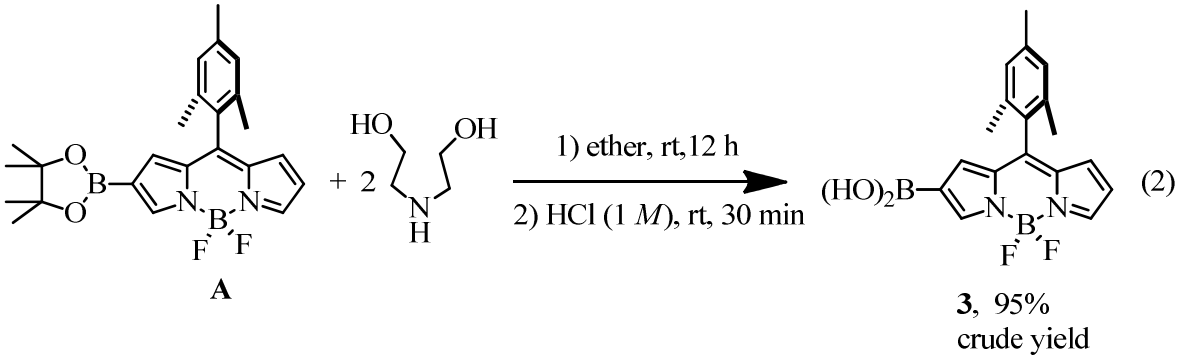

(2)

Boronic acid **3** was somewhat unstable and therefore, the crude product was prepared and rapidly used for the preparation of **4**.

The aim of attaching the mesityl fragment at the 8-position in one of the BODIPY monomers (red BODIPY moiety in Figure 1) was to ensure the probability of a high fluorescent quantum yield (Φ_{fl}) in the final products, due to restricted rotation of the 8-mesityl group to inhibit non-radiative relaxation pathways.[32] However, said position can be functionalized with other groups at an early stage either using the classic Lindsey methodology,[33] or the Liebeskind-Srogl cross-coupling reaction (LSCC).[34]

Indeed, dimer **4** displayed excellent reactivity in both LSCC and desulfitative reduction producing the desired products in 20 min or less. Arylboronic acids (with both electron-withdrawing and electron-rich groups), alkenyl, ferrocenyl, and heteroarylboronic acids reacted smoothly to give the corresponding products in high yields (compounds **5-14)**, regardless of their electronic properties or steric demands (Chart 1).

Chart 1. **LSCC and desulfitative reduction of dimer 4**.

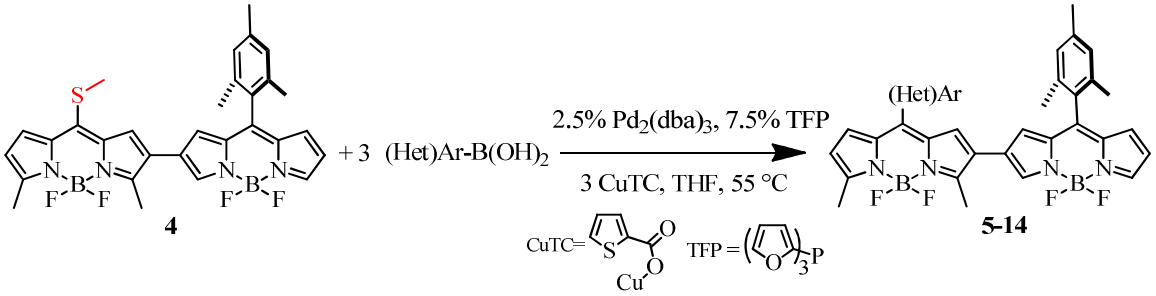

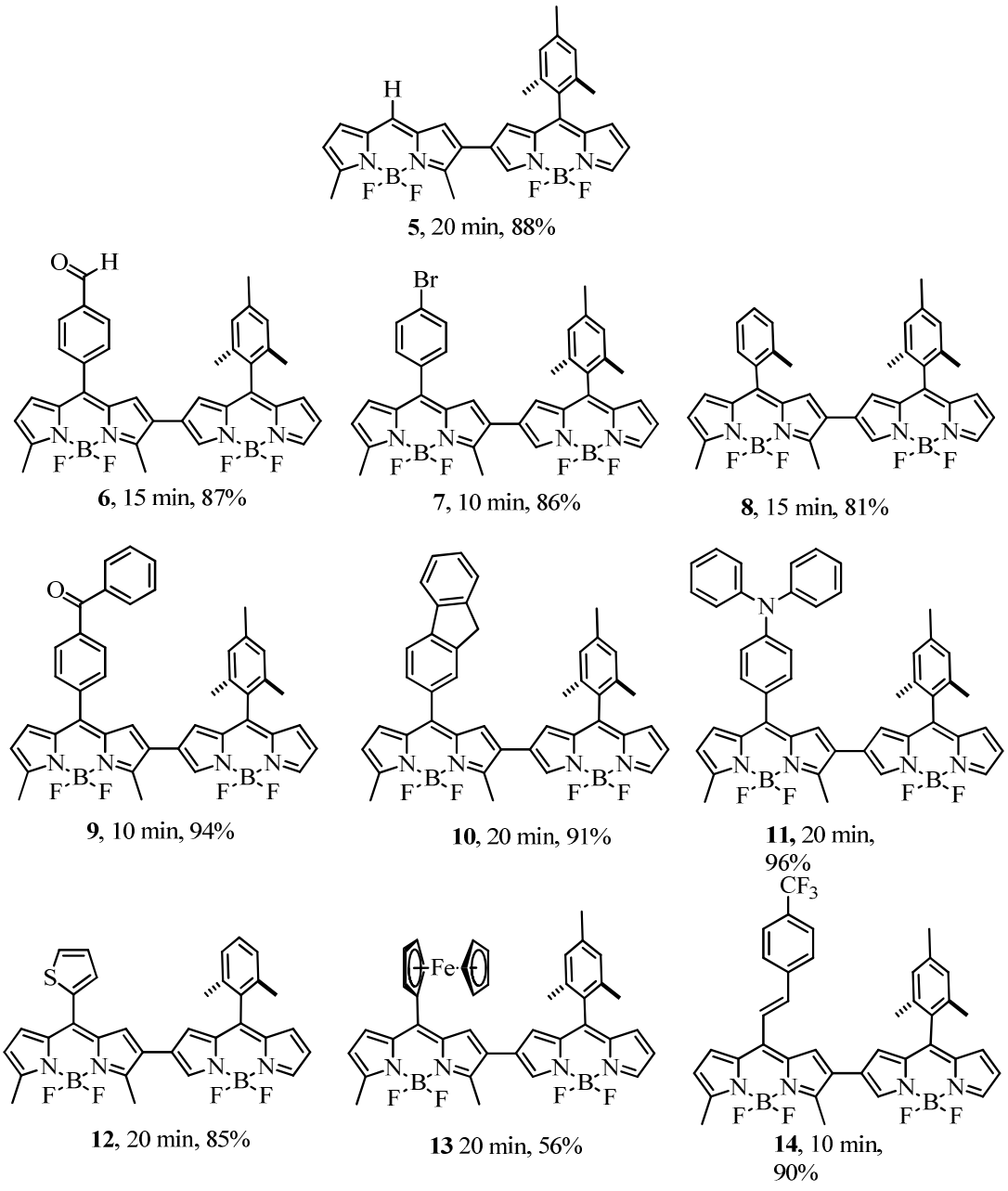

Conditions: **4** (1 equiv), (Het)Ar-B(OH)$_2$ or Et$_3$SiH (3 equiv), Pd$_2$(dba)$_3$ (2.5 mole %), TFP (7.5 mole %), THF, 55 °C

Dimer **4** also proved to be an excellent electrophilic partner in S$_N$Ar-like reactions with amines and phenols (Chart 2). Amine addition took place smoothly at rt in DCM to give 15-**17** in excellent yields. As in the case of the monomeric methylthioBODIPY, phenol addition needed CuTC as additive for the reaction to occur (compound **18** in Chart 2).[35]

This way, two important biomolecules, *i.e.*, estrone and δ-tocopherol, (compounds **19** and **20**, respectively) were labeled in a very straightforward manner.

Chart 2. **S_NAr-like reactions on dimer 4**

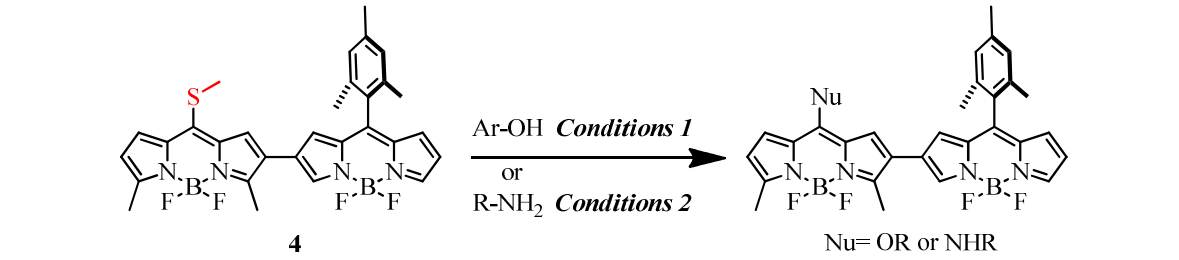

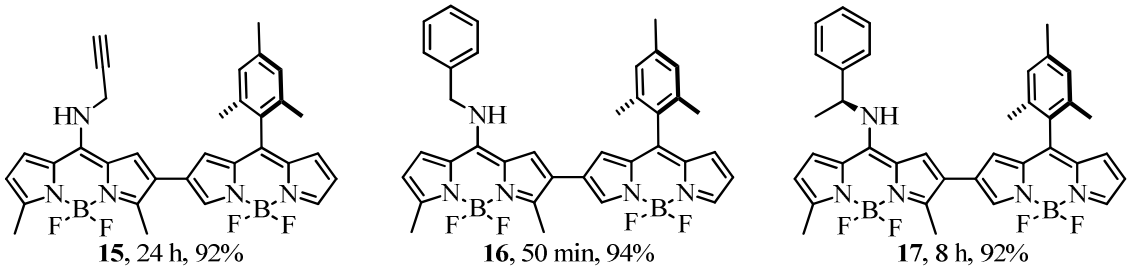

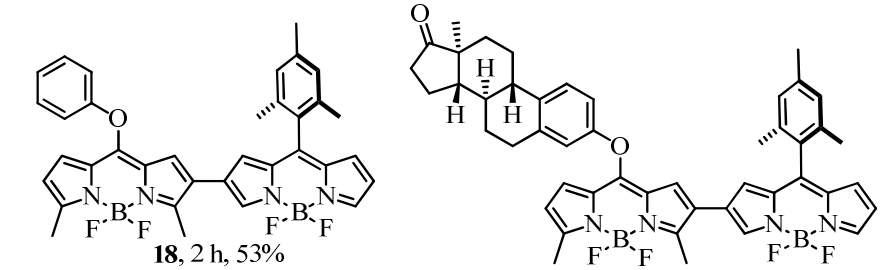

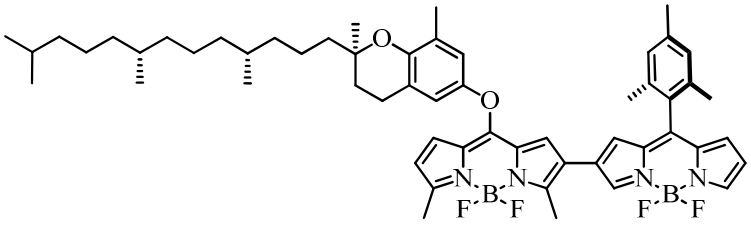

Conditions: 1:**4** (1 equiv), Ar-OH (10 equiv), CuTC (1.5 equiv), MeCN:DCM (1:1 v/v), 50 °C. Conditions 2: **4** (1 equiv), R-NH_2 (10 equiv), DCM, rt

X-ray structure of dimer 4. X-ray structure of **4** reveals a *trans* geometry between the two BODIPY fragments with a dihedral angle of 32° (Figure 3). The methylthio-substituted BODIPY fragment is planar whereas the mesityl-substituted BODIPY moiety is slightly saddled, and it is twisted an angle of 82º with respect to the BODIPY plane, because of the steric influence of the two methyl groups in the benzene unit. Note also that the boron atom in that BODIPY unit is 8° off the plane. In fact, theoretical simulations predict this conformation with very similar geometrical parameters as the most stable one. However, according to the calculations, several conformations could be likely allowed in liquid medium due to the low energy difference with respect to a *cis*-conformation through low energy barriers (see conformational analysis in ESI, Figure S1).

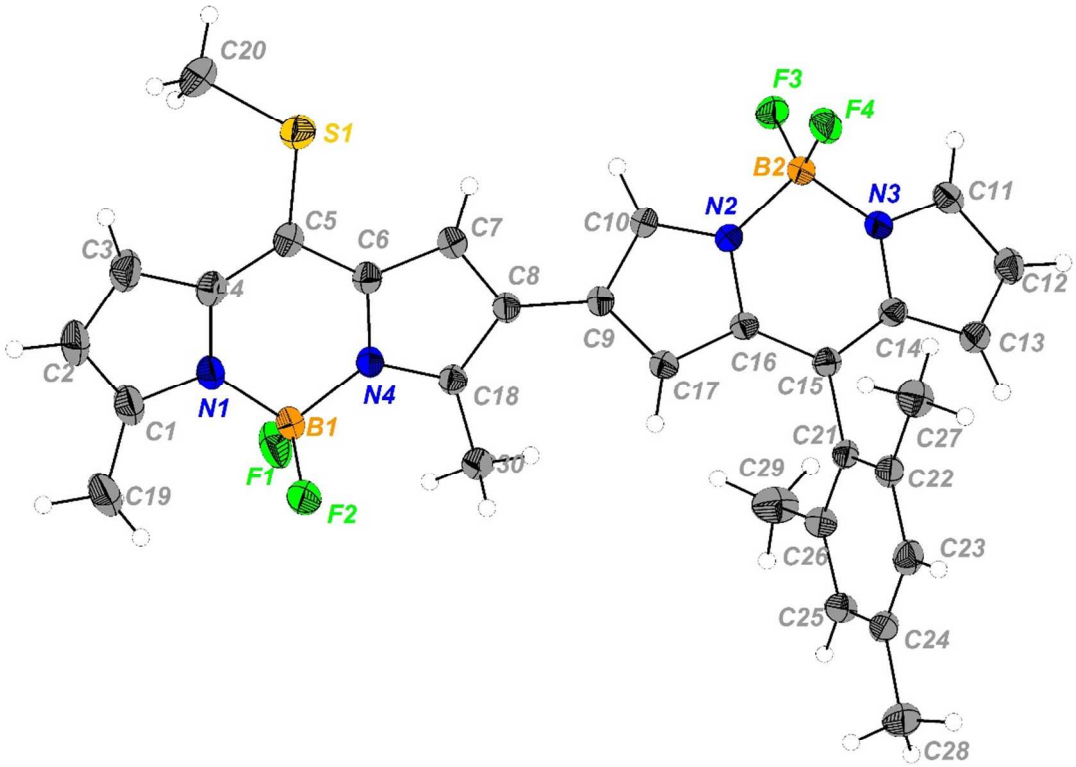

Figure 3. X-ray structure of **4** (ORTEP drawing, 50% probability)

Photophysical Study. A photophysical characterization was performed for all dimers in solvents with different polarity by absorption and fluorescence spectroscopy. The main photophysical properties of **4** are described in Table 1 and Figure 4.

Although the two BODIPY monomers are not in a coplanar disposition in **4**, the red-shifted absorption band observed in the dimer (λ_{abs} ~ 600 nm) with respect to the independent monomer units (λ_{abs} ~ 500 and 530 nm), is indicative of a π-electron delocalization between the two BODIPY moieties. Indeed, the dihedral angle between them does allow this electronic coupling (Figure 3 and Figure S1). Additionally, the band registered is relatively broad ($\Delta\nu \sim 2700$ cm^{-1}) with high molar absorption coefficients of around $\varepsilon \sim 11 \times 10^5$ M^{-1}cm^{-1} practically independent of the solvent (Table 1).

These experimental evidences are again in agreement with the quantum mechanical calculations (performed in c-hexane and ACN), which indicate the existence of two probable absorptions, assigned to the transitions HOMO→LUMO+1 and HOMO-1→LUMO, both showing a total delocalization along the units forming the dimer (Figure 4). Indeed, the contribution of these two transitions agrees well with the deconvolution into two Gaussian curves of the experimentally recorded main absorption band (Figure S2, Table ~~S1)~~).

Table 1. Photophysical properties of **4** in different solvents.

4	λ_{abs} nm	$\Delta\nu$ cm^{-1}	$\varepsilon \times 10^{-4}$ M^{-1}cm^{-1}	λ_{flu} nm	Φ_{flu}	τ ns
c-hexane	606	2651	11.04	652	0.83	2.67
toluene	607	2755	10.46	663	0.57	1.81
AcOEt	598	2772	10.92	664	0.19	0.97
Acetone	595	2767	10.61	694	≤0.01	0.39
ACN	592	2795	10.66	740	≤0.01	0.17
MeS-BDP[1]	530	1282	7.1	538	0.95	6.53
MesitylBDP[2]	503	463	7.7	515	0.82	5.68

[1] data in c-hexane;[36] [2]data in toluene[37]

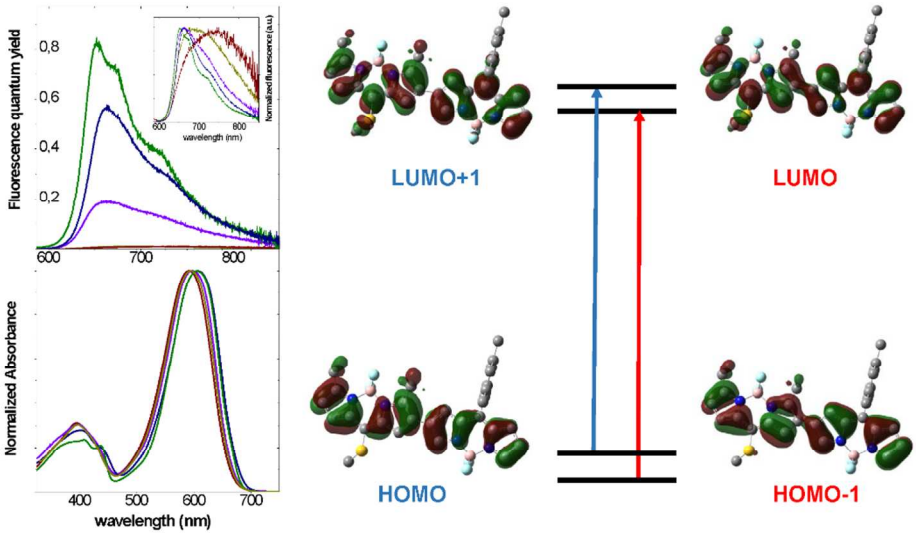

Figure 4. (left) Normalized Absorbance (down) and Fluorescence (up) spectra of **4** in cyclohexane (green), toluene (blue), ethyl acetate (violet), acetone (dark yellow), acetonitrile (wine) and (right) Energy diagram of the electronic levels and the corresponding orbitals involved of **4**.

Although the absorption spectra of **4** do not practically vary with the polarity of the solvent, important differences are found in the emission properties. In apolar solvents, such as cyclohexane, the emission band is placed at around 650 nm with high fluorescence efficiency (Φ_{flu} = 0.83, Table 1), assigned to the emission from S_1 state of the dimer. As the polarity of the solvent increases the fluorescence capacity decreases, being practically quenched for more polar solvents such as acetone or acetonitrile (Table 1). Moreover, the emission spectra are gradually red shifted, showing a broad band placed up to 740 nm in ACN, characteristic of an ICT (Intramolecular Charge Transfer) state. In this line, the fluorescence lifetime gradually decreases as the solvent polarity increases from 3 ns to 170ps (Table 1), indicative of the increase of non-radiative paths (*i.e.* internal conversion)

in highly stabilized ICT state, particularly in polar solvents, thereby reducing significantly the fluorescence quantum yield.

The effect on the photophysical properties of the different substituents at *meso* position in one of the BODIPY moieties is also analyzed (Table S4), taking as reference compound **5** without any substitution in the variable BODIPY moiety. Indeed, compound **5** shows similar properties as compound **4** (Table S4) and the substitution of aryl group at *meso* position (compounds **6**, **7** and **8**), independently of its electron donor/acceptor nature, does not practically induce any important change on the photophysical properties, (Table S4, Figure S3). For the other dimers with bulkier aromatic substituents (compounds **9**, **10**, **11**) or heterocyclic group (compound **12**), a decrease of the fluorescence efficiency, is observed (Table S4). Note also that the incorporation of ferrocenyl group (dimer **13**) completely quenched the fluorescence. In this line, although also a drastic quenching of the fluorescence quantum yield is observed in compound **14**, assigned to the free rotation of the styryl group, it is important to note that the extension of the π-conjugation by this substitution in one of the monomers is transmitted to the whole dimer, inducing a more important red-shift in the spectroscopic bands with respect to the other dimers (Table S4). This effect should be considered for the future design of dimers in the deep red or NIR region. Finally, the presence of heteroatoms at *meso* position in one of the BODIPY units (compounds **15**-**20**), induces a clear blue shift in the absorption band (Table 2, Table S5, Figure S4), particularly in amino derivates with higher electron donor ability (the Hammet parameters are σ_p^+ -1.81 and -0.50 for amino and phenoxy groups, respectively).

Table 2. Photophysical properties of dimers **15** and **18** in cyclohexane and ethyl acetate (AcOEt).

	λ_{abs} nm	$\Delta\nu$ cm^{-1}	$\varepsilon \times 10^{-4}$ $M^{-1}cm^{-1}$	λ_{flu}	Φ_{flu}	τ ns
Compound **15**						
c-hex	458/568	3280	4.31	633	0.42	2.30
AcOEt	477/568	3232	4.58	690	0.06	0.58
Compound **18**						

c-hex	582	2815	6.08	630	0.89	2.76
AcOEt	577	2868	5.88	665	0.16	0.92

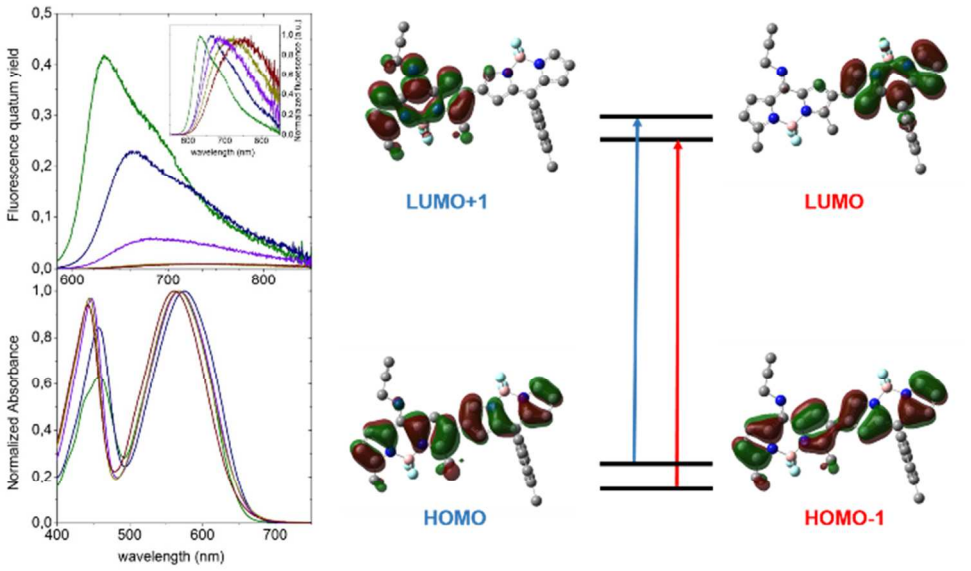

Figure 5. (Left) Height-normalized Absorbance (down) and Fluorescence spectra normalized to the quantum yield (height-normalized emission band is inset) (up) of dimer **15** in cyclohexane (green), toluene (blue), ethyl acetate (violet), acetone (dark yellow), acetonitrile (wine) and (right) Energy diagram of the electronic levels and the corresponding orbitals involved of dimer **15.**

DFT theory simulations predict for compound **15** a ground state delocalized through the two monomer units in the dimer whereas in the excited state the electron density localizes in only one of the fragments (see spatial distribution of the orbitals in Figure 5). Indeed, the more probable absorptions for compound **15** involve different transitions. The transitions responsible for the absorption in the blue region appear to be the HOMO→LUMO+1 (59% contribution) and the HOMO-1→LUMO (41%), while the HOMO→LUMO transition is responsible for the absorption in the green part of the Vis (Table S6). However, only the less energetic transition is responsible for the emission, which as in the other dimers, becomes broad, red-shifted and less intense because of the formation of an ICT state with the increasing of the solvent polarity. Similar behavior is found for dimers with oxygen-derivatives at *meso*-position (compound **18**-**20**), but their fluorescence efficiency remains slightly higher (Table S5, Figure S4), due to the weaker electron-donor character of the

oxygen in comparison to the nitrogen. Indeed, dimer **18,** although maintaining a similar spatial distribution of the orbitals as in the dimer **15**, does not show such a perfect localization in each BODIPY units (Figure S5).

Conclusions

In summary, a new route of synthesis of 2,6'-BODIPY dimers with high yields and short reaction times from a single, fully functionalizable building block is detailed. The resultant dimers show absorption bands at around 600 nm as a consequence of electronically coupled monomers disposed with a dihedral angle of around 30º. This conformation, elucidated by XRD was confirmed by DFT simulations. The incorporation of different aryl groups at *meso* position of one of the BODIPY units does not practically make any impact in the photophysical properties, whereas the attachment of heteroatoms produces important blue shifts in the absorption spectra. However, the emission properties in all the compounds are quite similar, obtaining the highest fluorescence efficiency in non-polar solvents, but in polar solvents an ICT state is activated producing red-shifted emission bands with poor emission efficiency. Further studies on the design of new dimers with emission bands in the red part of the visible spectrum will be carried out by the incorporation of π-conjugated groups in one or both BODIPY monomers. This methodology could conceptually be extended to the preparation of BODIPY trimers and other oligomers. We are actively exploring this possibility and the results will be disclosed in due course.

Experimental

Spectroscopic Characterization. The photophysical properties for all the compounds were measured in diluted solutions (approx. 5 x 10^{-6} M). The UV/vis absorption spectra were recorded on a Varian dual beam spectrometer (CARY 4E) in transmittance mode. Emission spectra were recorded on a spectrofuorimeter Edinburgh Instruments (FLSP920 model) with a xenon flash lamp 450 W as the excitation source. The fluorescence spectra were corrected from the wavelength dependence of the detector sensibility. Fluorescence quantum yield (Φ_{fl}) was obtained using as reference Nile Blue (Φ_{fl} = 0. 30 in methanol). The fluorescence lifetime decay curves were measured with the time correlated single-photon counting technique in the same spectrofluorimeter using a multichannel plate

detector (HamamatsuR38094–50) with picosecond time-resolution. Fluorescence decay curves were monitored at the maximum emission wavelength after excitation by means of a Fianium Supercontinuum laser with 150 ps full width at half maximum (FWHM) pulses. The fluorescence lifetime (t) was obtained after deconvolution of the instrumental response signal from the recorded decay curves by means of an iterative method. The goodness of the exponential fit was controlled by statistical parameters (chi square, χ^2, and analysis of the residuals).

Quantum mechanics calculations: Ground state geometries were optimized at the Density Functional Theory (DFT) using the hybrid B3LYP method, and the double valence basis set with a polarization function (6-31g*). The energy minimization was carried out without any geometrical constraints and an energy minimum was reached when the corresponding frequency analysis did not give any negative value. Absorption energies and probability were simulated with the Time Dependent (TD DFT) method using the same basis set. The conformational search was conducted at the same calculation level performing relaxed scans of 10º with regard to the dihedral angle between the BODIPYs planes of the dimer. The solvent effect (acetonitrile or cyclohexane) was taken into account in all the aforementioned calculations by means of the Polarizable Continuum Model (PCM). All the calculations were performed using the Gaussian 16 software as implemented in the computational cluster "arina" of the UPV/EHU.

X-ray Crystal Structure determination: Single crystals of compound **4** [$C_{30}H_{28}B_2F_4N_4S$] were obtained. A suitable crystal was selected and mounted on a SuperNova, which was equipped with monochromated Cukα radiation (λ= 1.54184 Å) and Atlas CCD detector. The crystal was kept at 150.00 K during data collection. Using Olex2,[38] the structure was solved with the ShelXS[39] structure solution program using Direct Methods and refined with the ShelXL[40] refinement package using Least Squares minimisation.

Synthesis and characterization: ^{1}H and ^{13}C NMR spectra were recorded in deuteriochloroform ($CDCl_3$), with either tetramethylsilane (TMS) (0.00 ppm ^{1}H, 0.00 ppm ^{13}C), chloroform (7.26 ppm ^{1}H, 77.00 ppm ^{13}C). Data are reported in the following order: chemical shift in ppm, multiplicities (br (broadened), s (singlet), d (doublet), t (triplet), q (quartet), m (multiplet), exch (exchangeable), app (apparent)), coupling constants, *J* (Hz), and integration. Infrared spectra were recorded on a FTIR spectrophotometer. Peaks are

reported (cm^{-1}) with the following relative intensities: s (strong, 67–100 %), m (medium, 40–67%), and w (weak, 20–40%). Melting points are not corrected. TLC was conducted in Silica gel on TLC Al foils. Detection was done by UV light (254 or 365 nm). HRMS samples were ionized by ESI+ and recorded via the TOF method.

Materials. Starting 3,5-dimethyl-8-(methylthio)BODIPY, CuTC, tri(2-furyl)phosphine, and boronic acids are commercially available. Solvents were dried and distilled before use.

Synthesis of 3. A round-bottom flask, equipped with a stir bar, was charged with pinacol boronic ester **A** (200.0 mg, 0.4586 mmol, 1 equiv.) and ethyl ether (20 mL). Diethanolamine (0.9172 mmol, 2 equiv.) was added and the solution was stirred for 12 h at room temperature. The precipitate was decanted and washed with ethyl ether. The precipitate was suspended in ethyl ether (20 mL), and 0.1 *M* HCl (20 mL) was added. The final solution was stirred by 30 min at room temperature. The organic phase was washed with brine (20 mL) and dried with magnesium sulfate, filtered, and evaporated under reduced pressure. Due to its instability, boronic acid **4** was used without further purification and prepared prior to its use. Compound **3** was obtained as an orange solid in 95% crude yield (154 mg).

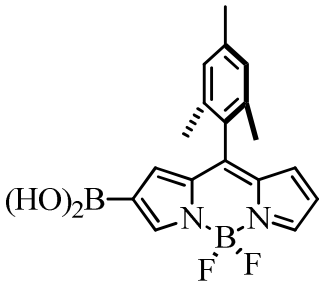

Synthesis of 2. A two-necked round-bottom flask was equipped with a stir-bar was purged with N_2 and charged with 8-methylthio-3,5-dimethylBODIPY (900 mg, 3.382 mmol, 1 equiv.), dry DMF (171 mL), and dry dichloromethane (171 mL). A solution of NBS (722 mg, 4.058 mmol, 1.2 equiv.) in dry DCM (100 mL) was added dropwise with an addition funnel at rt. The reaction mixture was stirred for 6 h, after which brine was added (400 mL). The organic phase is separated and washed with brine (2 x 150 mL). The aqueous phase was further extracted with EtOAc (2 x 150 mL). The organic phases were combined, dried with $MgSO_4$, filtered, and the solvent removed in vacuo. The product was purified by column chromatography (SiO_2-gel, EtOAc-hexanes gradient).

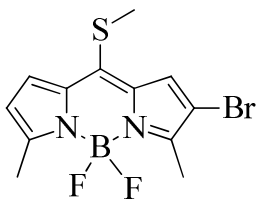

TLC (20% AcOEt/hexanes) R_f = 0.58, mp 134.4 – 135.1 °C, purple crystals, yield = 83% (969 mg). IR (KBr cm^{-1}) 459 (w), 754 (w), 766 (w), 882 (w), 994 (s), 1015 (s), 1076 (s), 1152 (s), 1267 (s), 1451 (s), 1478 (s), 1499 (s), 1539 (s). ^{1}H NMR (500 MHz, $CDCl_3$) δ 7.35 (d, *J* = 4.2 Hz, 1H), 7.28 (s, 1H), 6.32 (d, *J* = 4.3 Hz, 1H), 2.71 (s, 3H), 2.60 (s, 3H), 2.57 (s, 3H).^{13}C NMR (125 MHz, $CDCl_3$): δ 159.27, 152.36, 144.86, 135.84, 133.33, 129.79, 126.89, 120.55, 120.53, 107.36, 107.33, 21.59, 15.15, 13.23. HRMS (ESI+) *m*/*z* calcd for $C_{12}H_{13}BBrF_2N_2S$ $[M+H]^+$ 345.0045. Found 345.0041.

Synthesis of dimer 4. A dry Schlenk tube, equipped with a stir bar and a septum, was charged with BODIPY **2** (100 mg, 0.2896 mmol, 1 equiv.), freshly prepared boronic acid **3** (0.5791 mmol, 2 equiv.), $Pd(OAc)_2$ (0.0145 mmol, 0.05 equiv.), S-Phos (0.0362 mmol, 0.125 equiv.) and KOAc (1.014 mmol, 3.5 equiv.) under nitrogen. The tube was purged with N_2 three times. Toluene (10 mL) and water (100 μL) were added and the reaction mixture was stirred at 90 °C and stopped after BODIPY **2** was consumed (monitored by TLC, 20 minutes). The solvent was evaporated under reduced pressure. The compound was purified by column chromatography using SiO_2-gel and 10% EtOAc/hexanes as eluent.

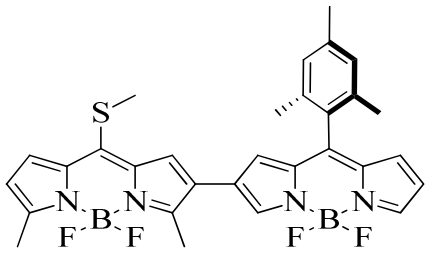

TLC (20% EtOAc/hexanes) R_f = 0.37, m.p. 270.0–271.5 °C, dark blue crystals, yield = 80% (132 mg). IR (KBr cm^{-1}) 706 (m), 730 (m), 769 (m), 983 (m), 997(m), 1024 (s), 1066 (s), 1103 (s), 1129 (s), 1175 (m), 1200 (m), 1248 (s), 1263 (s), 1319 (m), 1359 (s), 1399 (m), 1463 (m), 1529 (s), 1552 (s), 1611(w). ^{1}H NMR (500 MHz, $CDCl_3$) δ 8.09 (d, *J* = 5.4 Hz, 1H), 7.93 (s, 1H), 7.31 (d, *J* = 4.0 Hz, 1H), 7.29 (s, 1H), 6.99 (s, 1H), 6.68 (d, *J* = 3.2 Hz, 7H), 6.64 (s, 1H), 6.49 (d, *J* = 4.4 Hz, 1H), 6.30 (d, *J* = 4.1 Hz, 1H), 2.71 (s, 3H), 2.66 (s, 3H), 2.60 (s, 3H), 2.39 (s, 3H), 2.14 (s, 6H). ^{13}C NMR (125 MHz, $CDCl_3$) δ 158.14, 153.72, 147.29, 144.73, 144.11, 142.89, 139.16, 136.48, 135.97, 135.92, 135.84, 134.32, 130.43, 129.72, 128.93, 128.47, 127.12, 124.85, 124.73, 123.76, 119.99, 118.89, 21.83, 21.32, 20.21, 15.09, 14.43. HRMS (ESI+) *m*/*z* calcd for $C_{30}H_{29}B_2F_4N_4S$ $[M + H]^+$ 575.2240. Found 575.2231.

General procedure for Liebeskind-Srogl Cross Coupling Reaction (LSCC) and the desulfitative reduction involving dimer 4 (GP1). All reactions were carried out with 25 mg (0.0437 mmol, 1 equiv) of dimer **4** as limiting reagent and the other components of the reaction were added in the amounts stated in the GP1.

A dry Schlenk tube, equipped with a stir bar, was charged with dimer **4** (1 equiv.), the boronic acid or triethylsilane (3 equiv.) and dry THF (2 mL) under N_2. The stirred solution was sparged with N_2 for 10 minutes, whereupon CuTC (3 equiv.), $Pd_2(dba)_3$ (2.5 mol%), and TFP (7.5 mol%) were added under N_2. The reaction mixture was immersed into a pre-heated oil bath at 55 °C. After TLC showed that the reaction went to completion, the reaction mixture was allowed to reach room temperature, the solvent was removed in vacuo, and the product was purified by column chromatography using SiO_2-gel and EtOAc/hexanes as eluent.

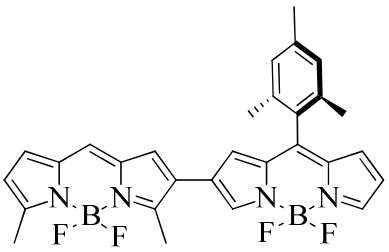

Dimer 5: According to GP1. TLC (20% EtOAc/hexanes) R_f = 0.17, m.p. 274.8-275.6 °C (dec), dark blue crystals, yield = 88% (20 mg). IR (KBr cm^{-1}) 420(w), 432(w), 633(m), 707(m), 767(m), 925(m), 983(s), 1005(s), 1066(s), 1102(s), 1167(m), 1248(s), 1265(s), 1361(s), 1397(s), 1467(m), 1554(s), 1606(s). ^{1}H NMR (500 MHz, $CDCl_3$) δ 8.07 (s, 1H), 7.93 (s, 1H), 7.03 (s, 1H), 6.99 (s, 2H), 6.96 (d, *J* = 4.1 Hz, 1H), 6.94 (s, 1H), 6.69 (d, *J* = 4.0 Hz, 1H), 6.63 (s, 1H), 6.51 – 6.46 (m, 1H), 6.29 (d, *J* = 4.1 Hz, 1H), 2.67 (s, 3H), 2.62 (s, 3H), 2.38 (s, 3H), 2.14 (s, 6H). ^{13}C NMR (125 MHz, $CDCl_3$) δ 159.73, 155.05, 147.29, 144.73, 142.84, 139.16, 136.46, 135.89, 135.84, 135.43, 133.52, 130.76, 130.44, 129.70, 128.46, 127.00, 126.56, 125.44, 125.19, 124.70, 120.38, 118.87, 21.31, 20.19, 15.16, 14.52. HRMS (ESI+) *m*/*z* calcd for $C_{29}H_{26}B_2F_4N_4$ [M] 528.2283. Found 528.2284.

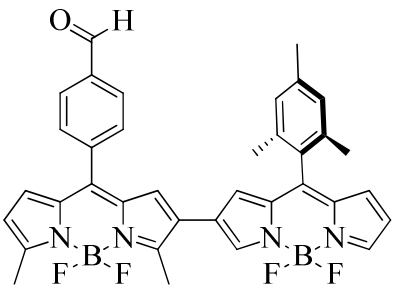

Dimer 6: According to GP1. TLC (20% EtOAc/hexanes) R_f = 0.12, m.p. 289.0-290.5 °C (dec), dark blue crystals, yield = 87% (24 mg). IR (KBr cm^{-1}) 705(w), 768(w),

777(w), 985(m), 1012(m), 1069(m), 1105(s), 1147(m), 1221(w), 1257(s), 1329(w), 1340(w), 1362(m), 1399(m), 1446(w), 1550(s), 1573(m), 1604(w), 1700(m), 3440(m). ^{1}H NMR (500 MHz, $CDCl_3$) δ 10.13 (s, 1H), 8.02 (d, *J* = 7.8 Hz, 3H), 7.92 (s, 1H), 7.67 (d, *J* = 8.0 Hz, 2H), 6.95 (s, 2H), 6.67 (d, *J* = 3.9 Hz, 2H), 6.63 (s, 1H), 6.58 (s, 1H), 6.48 (dd, *J* = 4.1, 1.6 Hz, 1H), 6.32 (d, *J* = 4.1 Hz, 1H), 2.73 (s, 3H), 2.67 (s, 3H), 2.37 (s, 3H), 2.11 (s, 6H). ^{13}C NMR (125 MHz, $CDCl_3$) δ 191.51, 159.83, 155.46, 147.32, 144.99, 142.55, 140.20, 139.92, 139.18, 137.38, 136.49, 135.98, 135.73, 134.73, 133.16, 131.09, 130.65, 130.60, 129.70, 129.66, 128.44, 126.79, 125.75, 125.51, 124.63, 120.69, 119.01, 116.03, 21.29, 20.16, 15.22, 14.60. HRMS (ESI+) *m*/*z* calcd. for $C_{36}H_{31}B_2F_4N_4O$ $[M+H]^+$ 633.2627. Found 633.2618.

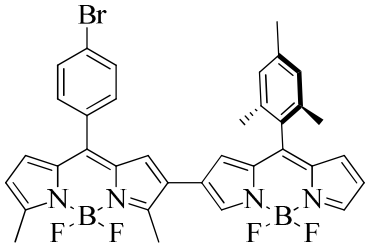

Dimer 7: According to GP1. TLC (20% EtOAc/hexanes) R_f = 0.34, m.p. 275.0-276.0 °C, dark blue crystals, yield = 86% (26 mg). IR (KBr cm^{-1}) 446(w), 433(w), 551(w), 679(w), 705(m), 740(m), 767(m), 883(m), 900(m), 933(m), 986(s), 1010(s), 1067(s), 1104(s), 1146(s), 1221(m), 1255(s), 1328(s), 1363(s), 1399(s), 1445(m), 1487(m), 1549(s), 1609(w). ^{1}H NMR (500 MHz, $CDCl_3$) δ 8.04 (s, 1H), 7.92 (s, 1H), 7.64 (d, *J* = 8.3 Hz, 2H), 7.37 (d, *J* = 8.3 Hz, 2H), 6.98 (s, 2H), 6.70 (d, *J* = 4.1 Hz, 1H), 6.67 (s, 2H), 6.59 (s, 1H), 6.48 (dd, *J* = 4.0, 1.4 Hz, 1H), 6.31 (d, *J* = 4.2 Hz, 1H), 2.72 (s, 3H), 2.66 (s, 3H), 2.38 (s, 3H), 2.12 (s, 6H). ^{13}C NMR (125 MHz, $CDCl_3$) δ 159.37, 154.90, 147.26, 144.81, 142.69, 140.73, 139.14, 136.48, 135.92, 135.75, 134.80, 133.23, 132.94, 131.89, 131.83, 130.71, 130.48, 129.71, 128.44, 126.99, 125.58, 125.42, 124.81, 124.62, 120.44, 118.91, 21.31, 20.18, 15.18, 14.56. HRMS (ESI+) *m*/*z* calcd. for $C_{35}H_{29}B_2BrF_4N_4Na$ $[M+Na]^+$ 706.1597. Found 706.1617.

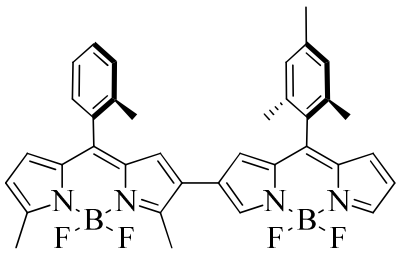

Dimer 8: According to GP1. TLC (20% EtOAc/hexanes) R_f = 0.48, m.p. 299.5-300.2 °C, dark blue crystals, yield = 81% (22 mg). IR (KBr cm^{-1}) 438(m), 704(s), 740(s), 765(m), 771(m), 882(m), 931(m), 983(s), 1008(s), 1067(s), 1102(s), 1132(s), 1217(m), 1261(s), 1362(s), 1397(s), 1466(s),

1555(s), 1648(w). ^{1}H NMR (500 MHz, $CDCl_3$) δ 8.01 (s, 1H), 7.90 (s, 1H), 7.40 (td, *J* = 7.5, 1.4 Hz, 1H), 7.34 – 7.28 (m, 1H), 7.27 (d, *J* = 6.5 Hz, 1H), 7.23 (dd, *J* = 7.5, 1.2 Hz, 1H), 6.97 (s, 2H), 6.65 (d, *J* = 4.0 Hz, 1H), 6.56 (s, 1H), 6.51 (d, *J* = 4.1 Hz, 1H), 6.49 – 6.44 (m, 2H), 6.25 (d, *J* = 4.1 Hz, 1H), 2.72 (s, 3H), 2.66 (s, 3H), 2.37 (s, 3H), 2.22 (s, 3H), 2.11 (s, 6H). ^{13}C NMR (125 MHz, $CDCl_3$) δ 159.18, 154.53, 147.17, 144.56, 142.92, 141.81, 139.10, 136.71, 136.45, 135.79, 135.49, 133.82, 133.31, 130.45, 130.30, 130.08, 129.71, 129.45, 128.44, 127.23, 125.42, 125.23, 125.07, 124.58, 120.23, 118.78, 21.30, 20.17, 15.17, 14.56. HRMS (ESI+) *m*/*z* calcd. for $C_{36}H_{33}B_2F_4N_4$ $[M+H]^+$ 619.2817. Found 619.2834.

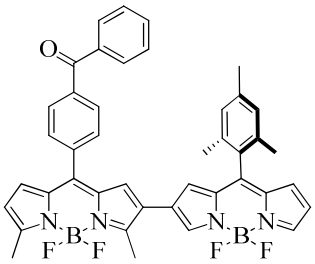

Dimer 9: According to GP1. TLC (20% EtOAc/hexanes) R_f = 0.18, m.p. 172.2-174.1 °C, dark blue crystals, yield = 94% (29 mg). IR (KBr cm^{-1}) 706(m), 986(m), 1013(m), 1068(m), 1103(s), 1145(m), 1256(s), 1361(m), 1399(m), 1466(m), 1555(s), 1662(m). ^{1}H NMR (500 MHz, $CDCl_3$) δ 8.05 (s, 1H), 7.94 (d, *J* = 1.7 Hz, 1H), 7.93 (dd, *J* = 3.6, 1.8 Hz, 2H), 7.89 (t, *J* = 3.1 Hz, 1H), 7.88 (d, *J* = 1.4 Hz, 1H), 7.67 – 7.59 (m, 3H), 7.58 – 7.51 (m, 2H), 6.98 (s, 2H), 6.74 (d, *J* = 4.2 Hz, 1H), 6.71 (s, 1H), 6.67 (d, *J* = 4.1 Hz, 1H), 6.60 (s, 1H), 6.48 (dd, *J* = 4.2, 1.7 Hz, 1H), 6.33 (d, *J* = 4.2 Hz, 1H), 2.74 (s, 3H), 2.67 (s, 3H), 2.37 (s, 3H), 2.12 (s, 6H). ^{13}C NMR (125 MHz, $CDCl_3$) δ 195.99, 159.62, 155.22, 147.34, 144.87, 142.73, 140.75, 139.18, 139.11, 137.95, 137.19, 136.48, 135.96, 135.79, 134.88, 133.27, 133.04, 130.83, 130.54, 130.42, 130.25, 130.02, 129.71, 128.67, 128.48, 126.94, 125.66, 124.67, 120.57, 118.93, 21.31, 20.18, 15.21, 14.58. HRMS (ESI+) *m*/*z* calcd. for $C_{42}H_{34}B_2F_4N_4ONa$ $[M+Na]^+$ 731.2748. Found 731.2761.

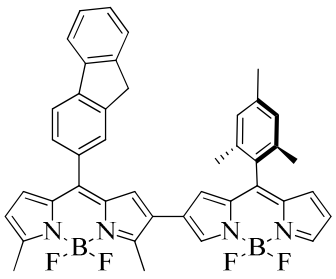

Dimer 10: According to GP1. TLC (20% EtOAc/hexanes) R_f = 0.33, m.p. 202.2-203-5 °C, dark blue crystals, yield = 91% (28 mg). IR (KBr cm^{-1}) 704(w), 764(w), 1013(m), 1069(m), 1106(s), 1259(s), 1362(m), 1399(m), 1464(m), 1549(s), 1612(w), 3453(m). ^{1}H NMR (500 MHz, $CDCl_3$) δ 8.05 (s, 1H), 7.93 – 7.89 (m, 2H), 7.87 (d, *J* = 7.4 Hz, 1H), 7.67 (d, *J* = 0.5

Hz, 1H), 7.61 (d, *J* = 7.4 Hz, 1H), 7.52 (dt, *J* = 9.2, 4.6 Hz, 1H), 7.45 (td, *J* = 13.6, 6.6 Hz, 1H), 7.39 (td, *J* = 7.4, 1.1 Hz, 1H), 6.95 (s, 2H), 6.80 (d, *J* = 4.1 Hz, 1H), 6.77 (s, 1H), 6.65 (d, *J* = 4.1 Hz, 1H), 6.59 (s, 1H), 6.46 (dd, *J* = 4.1, 1.7 Hz, 1H), 6.31 (d, *J* = 4.2 Hz, 1H), 4.01 (d, *J* = 5.0 Hz, 2H), 2.74 (s, 3H), 2.68 (s, 3H), 2.35 (s, 3H), 2.11 (s, 6H). ^{13}C NMR (125 MHz, $CDCl_3$) δ 158.66, 154.09, 147.15, 144.51, 144.05, 143.82, 143.35, 143.04, 140.76, 139.08, 136.46, 135.83, 135.20, 133.62, 132.45, 131.06, 130.27, 129.72, 129.65, 128.43, 127.88, 127.36, 127.25, 127.16, 125.92, 125.38, 124.97, 124.64, 120.60, 120.09, 119.80, 118.73, 37.14, 21.28, 20.18, 15.17, 14.52. HRMS (ESI+) *m*/*z* calcd. for $C_{42}H_{35}B_2F_4N_4$ $[M+H]^+$ 696.2977. Found 693.2992.

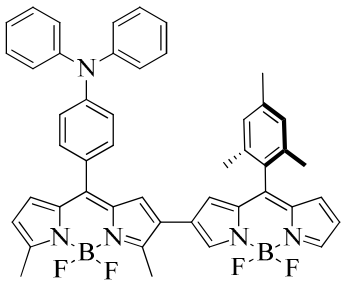

Dimer 11: According to GP1. TLC (20% EtOAc/hexanes) R_f = 0.54, m.p. 155.5-157.0 °C, dark purple crystals, yield = 96% (31 mg). IR (KBr cm^{-1}) 415(m), 442(m), 509(m), 549(m), 704(s), 744(s), 765(s), 831 (m), 883(m), 901(m), 933(m), 986(s), 1014(s), 1068(s), 1104(s), 1223(s), 1258(s), 1330(s), 1360(s), 1399(s), 1465(s), 1492(s), 1555(s), 1588(s), 1735(m), 1608(m). ^{1}H NMR (500 MHz, $CDCl_3$) δ 8.09 (s, 1H), 7.91 (s, 1H), 7.40 – 7.31 (m, 6H), 7.25 – 7.19 (m, 4H), 7.15 (t, *J* = 7.4 Hz, 2H), 7.12 – 7.07 (m, 2H), 6.99 (s, 2H), 6.87 (d, *J* = 6.2 Hz, 2H), 6.66 (d, *J* = 4.0 Hz, 1H), 6.62 (s, 1H), 6.48 (dd, *J* = 4.1, 1.7 Hz, 1H), 6.31 (d, *J* = 4.2 Hz, 1H), 2.70 (s, 3H), 2.65 (s, 3H), 2.39 (s, 3H), 2.14 (s, 6H). ^{13}C NMR (125 MHz, $CDCl_3$) δ 157.89, 153.37, 150.32, 147.07, 146.90, 144.30, 143.49, 142.80, 139.12, 136.51, 135.96, 135.80, 134.92, 133.31, 131.91, 130.85, 130.14, 129.80, 128.46, 127.64, 126.58, 125.97, 125.71, 124.56, 120.47, 119.77, 118.65, 21.31, 20.19, 15.09, 14.37. HRMS (ESI+) *m*/*z* calcd. for $C_{47}H_{40}B_2F_4N_5$ $[M+H]^+$ 772.3404. Found 772.3415.

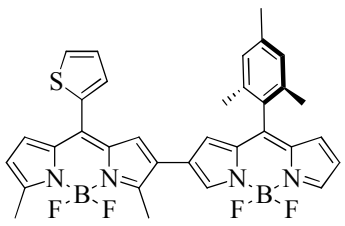

Dimer 12: According to GP1. TLC (20% EtOAc/hexanes) R_f = 0.21, m.p. 284.6-285.5 °C, dark blue crystals, yield = 85% (23 mg). IR (KBr cm^{-1}) 431(w), 442(w), 546(w), 704(s), 765(s), 931(s), 983(s), 1014(s), 1067(s), 1107(s), 1146(s), 1252(s), 1335(s), 1362(s), 1399(s), 1443(s), 1463(s), 1489(s), 1551(s), 1610(w), 3111(w). ^{1}H NMR (500 MHz, $CDCl_3$) δ 7.62 (dd, *J* = 5.1, 1.1 Hz, 1H),

7.44 (dd, *J* = 3.6, 1.1 Hz, 1H), 7.22 (dd, *J* = 5.1, 3.6 Hz, 1H), 7.07 (d, *J* = 4.2 Hz, 1H), 7.05 (s, 1H), 6.98 (s, 2H), 6.67 (d, *J* = 4.0 Hz, 1H), 6.62 (s, 1H), 6.48 (dd, *J* = 4.0, 1.5 Hz, 1H), 6.33 (d, *J* = 4.2 Hz, 1H), 2.71 (s, 3H), 2.66 (s, 3H), 2.38 (s, 3H), 2.14 (s, 6H). ^{13}C NMR (125 MHz, $CDCl_3$) δ 158.94, 154.49, 147.23, 144.62, 143.03, 139.13, 136.47, 135.85, 134.68, 134.58, 133.13, 131.92, 131.08, 130.36, 129.97, 129.72, 128.45, 127.98, 127.22, 125.96, 125.15, 124.64, 120.23, 118.81, 21.31, 20.19, 15.19, 14.53. HRMS (ESI+) *m*/*z* calcd. for $C_{33}H_{29}B_2F_4N_4S$ $[M+H]^+$ 611.2234. Found 611.2241.

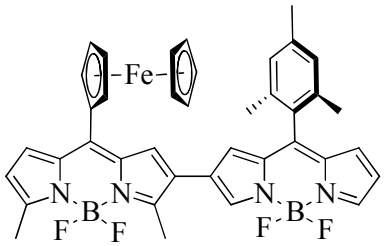

Dimer 13: According to GP1. TLC (20% EtOAc/hexanes) R_f = 0.21, m.p. 245.2-246.4 °C, dark blue crystals, yield = 56% (17 mg). IR (KBr cm^{-1}) 414(w), 430(w), 445(w), 481(w), 497(w), 707(m), 741(m), 764(m), 985(s), 1015(s), 1065(s), 1096(s), 1152(s), 1255(s), 1340(m), 1359(s), 1398(s), 1465(s), 1541(s), 1566(s), 1613(w), 3435(w). ^{1}H NMR (500 MHz, $CDCl_3$) δ 8.11 (s, 1H), 7.92 (s, 1H), 7.65 (d, *J* = 4.1 Hz, 1H), 7.48 (s, 1H), 6.99 (s, 2H), 6.67 (d, *J* = 4.0 Hz, 1H), 6.63 (s, 1H), 6.48 (dd, *J* = 4.0, 1.5 Hz, 1H), 6.31 (d, *J* = 4.2 Hz, 1H), 4.86 (t, *J* = 1.8 Hz, 2H), 4.65 (t, *J* = 1.8 Hz, 2H), 4.18 (s, 5H), 2.62 (s, 3H), 2.58 (s, 3H), 2.39 (s, 3H), 2.15 (s, 6H). ^{13}C NMR (125 MHz, $CDCl_3$) δ 155.91, 151.76, 147.12, 145.39, 144.36, 143.30, 139.12, 136.50, 135.99, 135.82, 134.81, 133.44, 130.21, 129.92, 129.77, 128.47, 127.75, 125.35, 124.53, 123.96, 119.07, 118.69, 79.79, 73.75, 71.63, 71.13, 21.33, 20.23, 15.10, 14.33. HRMS (ESI+) *m*/*z* calcd. for $C_{39}H_{34}B_2F_4FeN_4$ [M] 712.2265. Found 712.2263.

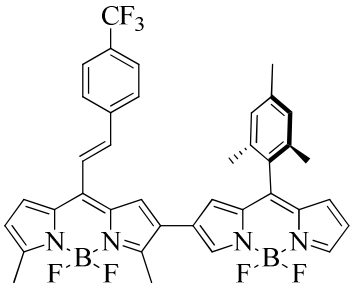

Dimer 14: According to GP1. TLC (20% EtOAc/hexanes) R_f = 0.39, m.p. 246.0–247.5 °C, dark green crystals, yield = 90% (27 mg). IR (KBr cm^{-1}) 706(m), 769 (m), 8221 (m), 956 (m), 985(m), 1015(s), 1043 (m), 1067(s), 1109(s), 1168(s), 1255(s), 1324(s), 1362(s), 1401(s), 1443(m), 1466(m), 1494(m), 1551(s), 1613(m), 1628(m). ^{1}H NMR (500 MHz,

$CDCl_3$) δ 8.09 (s, 1H), 7.93 (s, 1H), 7.71 – 7.65 (m, 4H), 7.36 (d, *J* = 16 Hz, 1H), 7.30 (d, *J* = 16 Hz, 1H), 7.16 (d, *J* = 4.1 Hz, 1H), 7.14 (s, 1H), 6.99 (s, 2H), 6.68 (d, *J* = 4.0 Hz, 1H), 6.65 (s, 1H), 6.49 (dd, *J* = 4.1, 1.6 Hz, 1H), 6.32 (d, *J* = 4.2 Hz, 1H), 2.70 (s, 3H), 2.64 (s, 3H), 2.38 (s, 3H), 2.14 (s, 6H). ^{13}C NMR (125 MHz, $CDCl_3$) δ 158.76, 154.25, 147.25, 144.81, 142.85, 140.28, 139.19, 137.68, 136.52, 135.94, 135.83, 133.97, 132.48, 131.62, 131.36, 130.48, 129.76, 128.46, 128.28, 127.87, 127.14, 126.16, 126.13, 125.11, 124.90, 123.71, 123.08, 119.95, 118.92, 21.30, 20.19, 15.19, 14.53. HRMS (ESI+) *m*/*z* calcd. for $C_{38}H_{31}B_2F_7N_4Na$ $[M+Na]^+$ 721.2528. Found 721.2518.

General procedure for the nucleophilic substitution involving dimer 4 with amines (GP2). In a round-bottom flask, equipped with a stir-bar under N_2, was placed dimer **4** (25 mg, 0.044 mmol, 1 equiv) and dry dichloromethane (DCM, 3 mL). CuTC (8.3 mg, 0.0655 mmol, 1 equiv) and the corresponding amine (0.437 mmol, 10 equiv) were added sequentially. The reaction mixture was stirred at rt until TLC shows the disappearance of **4**. The solvent was then removed in vacuo, and the product was isolated using Flash chromatography (SiO_2-gel, EtOAc/hexanes gradient).

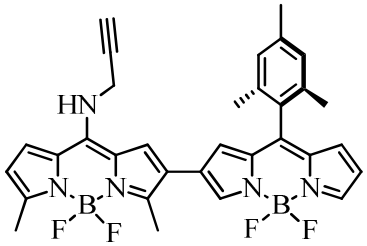

According to GP2. Compound 15: TLC (20% AcOEt/hexanes) R_f = 0.11, mp = 263.3 - 264.8 °C, dark purple crystals, yield = 92% (23 mg). IR (KBr cm^{-1}): 411(w), 430(w), 439(w), 652(w), 707(m), 726(m), 768(m), 934(m), 954(s), 985(s), 1068(s), 1106(s), 1155(s), 1251(s), 1311(s), 1361(s), 1401(s), 1437(s), 1472(s), 1551(s), 1719(m), 3113(w), 3284(w), 3315(w), 3419(w). ^{1}H NMR (500 MHz, $CDCl_3$): δ 8.06 (s, 1H), 7.90 (s, 1H), 6.99 (d, *J* = 5.9 Hz, 3H), 6.94 (s, 1H), 6.65 (d, *J* = 4.0 Hz, 1H), 6.61 (s, 1H), 6.47 (dd, *J* = 4.1, 1.8 Hz, 1H), 6.31 (t, *J* = 5.4 Hz, 1H), 6.22 (d, *J* = 4.0 Hz, 1H), 4.34 (dd, *J* = 5.4, 2.4 Hz, 2H), 2.60 (s, 3H), 2.55 (s, 3H), 2.48 (t, *J* = 2.4 Hz, 1H), 2.38 (s, 3H), 2.15 (s, 6H). ^{13}C NMR (125 MHz, $CDCl_3$): δ 149.79, 146.87, 144.98, 144.71, 143.85, 143.71, 139.07, 136.52, 136.02, 135.65, 129.86, 128.45, 124.62, 122.79, 121.13, 118.42, 116.43, 75.21, 36.91, 21.31, 20.20, 14.38, 13.61. HRMS (ESI+) *m*/*z* calcd for $C_{32}H_{29}B_2F_4N_5Na$ $[M+Na]^+$ 604.2433. Found 604.2448.

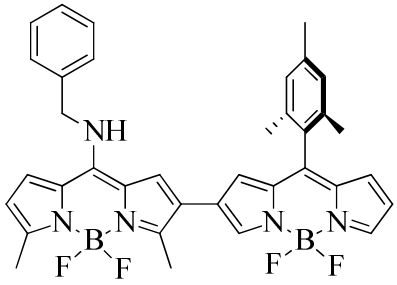

According to GP2. Compound 16. TLC (20% AcOEt/hexanes) R_f = 0.21, mp = 267.3 - 268.5 °C, dark purple crystals, yield = 94% (26 mg). IR (KBr cm^{-1}): 705(w), 730(w), 766(w), 953(m), 979(m), 1066(s), 1107(s), 1166(s), 1253(s), 1354(m) 1399(m), 1442(m), 1476(m), 1553(s), 1577(s), 3396(w). ^{1}H NMR (500 MHz, $CDCl_3$): δ 8.07 (s, 1H), 7.88 (s, 1H), 7.49 – 7.40 (m, 3H), 7.40 – 7.35 (m, 2H), 6.97 (s, 3H), 6.92 (s, 1H), 6.63 (d, *J* = 4.0 Hz, 1H), 6.60 (s, 1H), 6.45 (dd, *J* = 4.1, 1.8 Hz, 1H), 6.23 (d, *J* = 3.6 Hz, 1H), 6.16 (t, *J* = 4.8 Hz, 1H), 4.80 (d, *J* = 5.0 Hz, 2H), 2.62 (s, 3H), 2.58 (s, 3H), 2.37 (s, 3H), 2.13 (s, 6H). ^{13}C NMR (125 MHz, $CDCl_3$): δ 146.77, 145.33, 143.75, 139.03, 136.55, 136.01, 135.60, 135.39, 129.90, 129.77, 129.28, 128.42, 128.29, 124.56, 118.35, 51.97, 21.31, 20.20, 13.59. HRMS (ESI+) *m*/*z* calcd for $C_{36}H_{33}B_2F_4N_5Na$ $[M+Na]^+$ 656.2744. Found 556.2762.

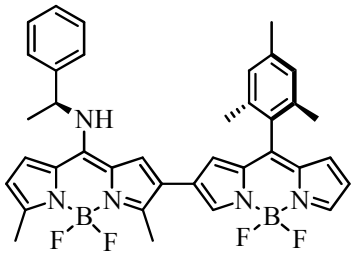

According to GP2. Compound 17. TLC (20% AcOEt/hexanes) R_f = 0.29, mp = 168.0 - 170.0 °C, dark purple crystals, yield = 92% (26 mg). IR (KBr cm^{-1}): 412(w), 432(w), 705(s), 728(m), 767(m), 968(s), 1067(s), 1104(s), 1167(s), 1252(s), 1282(s), 1359(s), 1400(s), 1436(s), 1472(s), 1555(s), 3375(m). ^{1}H NMR (500 MHz, $CDCl_3$): δ 8.04 (s, 1H), 7.88 (s, 1H), 7.37 (t, *J* = 6.1 Hz, 2H), 7.33 - 7.29 (m, 3H), 7.00 (s, 2H), 6.92 (s, 1H), 6.88 (d, *J* = 4.0 Hz, 1H), 6.65 (d, *J* = 3.8 Hz, 1H), 6.56 (s, 1H), 6.46 (d, *J* = 2.4 Hz, 1H), 6.25 (d, *J* = 7.3 Hz, 1H), 6.16 (d, *J* = 4.0 Hz, 1H), 5.22 (p, *J* = 6.6 Hz, 1H), 2.60 (s, 3H), 2.55 (s, 3H), 2.39 (s, 3H), 2.14 (d, *J* = 6.1 Hz, 6H), 1.76 (d, *J* = 6.6 Hz, 3H). ^{13}C NMR (125 MHz, $CDCl_3$): δ 146.72, 144.83, 143.73, 143.67, 141.17, 139.02, 136.56, 136.00, 135.57, 129.90, 129.72, 129.61, 128.43, 128.40, 125.42, 124.53, 118.36, 56.15, 24.56, 21.32, 20.21, 20.19, 14.38, 13.56. HRMS (ESI+) *m*/*z* calcd for $C_{37}H_{35}B_2F_4N_5$ [M] 647.3023. Found 647.3021.

General procedure for the nucleophilic substitution involving dimer 4 with phenols (GP3). In a round-bottom flask, equipped with a stir-bar under N_2, was placed

dimer **4** (25 mg, 0.044 mmol, 1 equiv) and dry acetonitrile (1.5 mL) and dry DCM (1.5 mL). CuTC (12.5 mg, 0.0655 mmol, 1.5 equiv) and the corresponding phenol (0.437 mmol, 10 equiv) were added sequentially. The reaction mixture was stirred at 50 °C until TLC shows **4** was consumed. The solvent was then removed in vacuo, and the product was isolated using Flash chromatography (SiO_2-gel, EtOAc/hexanes gradient).

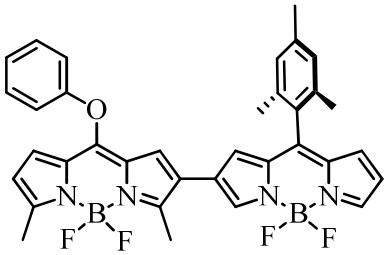

According to GP3. Compound 18. TLC (20% AcOEt/hexanes) R_f = 0.54, mp = 258.6 - 259.5 °C, dark purple crystals, yield = 53% (14 mg). IR (KBr cm^{-1}): 412(w), 431(w), 693(m), 704(m), 765(m), 776(m), 960(m), 986(m), 1013(s), 1069(s), 1100(s), 1149(s), 1253(s), 1271(s), 1365(m), 1401(m), 1467(m), 1488(m), 1559(s), 1736(w). ^{1}H NMR (500 MHz, $CDCl_3$): δ 7.98 (s, 1H), 7.91 (s, 1H), 7.46 – 7.39 (m, 2H), 7.29 – 7.28 (m, 1H), 7.20 – 7.13 (m, 2H), 6.97 (s, 2H), 6.83 (s, 1H), 6.67 (d, *J* = 4.0 Hz, 1H), 6.59 (s, 1H), 6.52 – 6.44 (m, 2H), 6.13 (d, *J* = 4.2 Hz, 1H), 2.65 (s, 3H), 2.59 (s, 3H), 2.37 (s, 3H), 2.12 (s, 6H). ^{13}C NMR (125 MHz, $CDCl_3$): δ 157.35, 156.13, 154.59, 151.72, 147.22, 144.50, 143.04, 139.12, 136.45, 135.87, 130.44, 130.28, 129.72, 128.45, 127.46, 127.34, 126.93, 126.42, 125.91, 124.82, 123.70, 121.28, 119.16, 118.76, 21.30, 20.18, 14.82, 14.19. HRMS (ESI+) *m*/*z* calcd for $C_{35}H_{31}B_2F_4N_4O$ $[M+H]^+$ 621.2608. Found 621.2626.

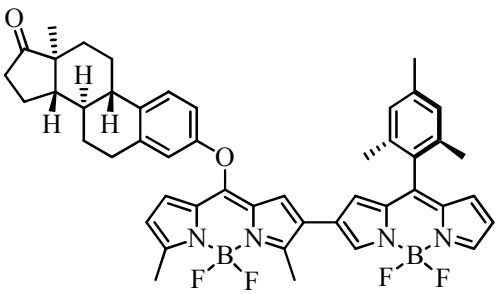

According to GP3. Compound 19. TLC (20% AcOEt/hexanes) R_f = 0.18, mp = 110.5 - 111.9 °C, dark purple solid, yield = 96% (33 mg). IR (KBr cm^{-1}): 706(m), 767(w), 964(m), 980(m), 1019(m), 1068(m), 1102(s), 1139(s), 1253(s), 1343(m), 1364(m), 1399(m), 1466(m), 1488(m), 1556(s), 1739(m), 2847(w), 2922(m), 3433(w). ^{1}H NMR (500 MHz, $CDCl_3$): δ 7.98 (s, 1H), 7.90 (s, 1H), 7.30 (d, *J* = 8.6 Hz, 1H), 6.97 (s, 2H), 6.93 (dd, *J* = 8.5, 2.5 Hz, 1H), 6.87 (d, *J* = 2.3 Hz, 1H), 6.85 (s, 1H), 6.66 (d, *J* = 4.0 Hz, 1H), 6.59 (s, 1H), 6.57 (d, *J* = 4.2 Hz, 1H), 6.47

(d, *J* = 3.0 Hz, 1H), 6.14 (d, *J* = 4.2 Hz, 1H), 2.89 (dd, *J* = 8.6, 3.8 Hz, 2H), 2.64 (s, 3H), 2.59 (s, 3H), 2.52 (dd, *J* = 19.1, 8.7 Hz, 1H), 2.37 (s, 3H), 2.35 – 2.29 (m, 1H), 2.17 (t, *J* = 4.6 Hz, 1H), 2.12 (s, 6H), 2.04 (s, 1H), 1.66 – 1.48 (m, 8H), 1.29 (d, *J* = 6.5 Hz, 1H), 0.95 (s, 3H). ^{13}C NMR (125 MHz, $CDCl_3$): δ 220.71, 156.02, 155.49, 154.70, 151.56, 147.19, 144.49, 143.12, 139.24, 139.13, 137.51, 136.45, 135.89, 135.83, 130.29, 129.72, 128.46, 127.69, 127.43, 127.23, 127.03, 126.43, 124.71, 121.24, 118.74, 116.14, 50.64, 48.10, 44.25, 38.19, 35.99, 31.71, 29.85, 26.41, 25.98, 21.75, 21.31, 20.19, 14.84, 14.06. HRMS (ESI+) *m*/*z* calcd for $C_{47}H_{47}B_2F_4N_4O_2$ $[M+H]^+$ 797.3824. Found 797.3831.

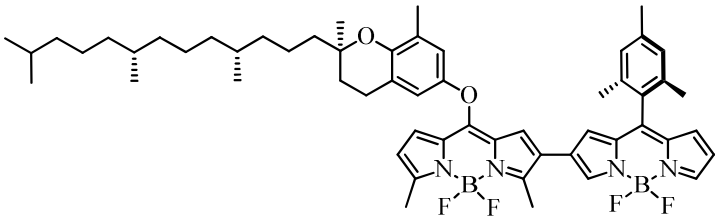

According to GP3. Compound 20. TLC (20% AcOEt/hexanes) R_f = 0.70, purple oil, yield = 25% (10 mg). IR (KBr cm^{-1}): 704(w), 1019(w), 1105(m), 1252(m), 1375(w), 1397(w), 1466(m), 1557(m), 1737(m), 2847(s), 2916(s), 3433(m). ^{1}H NMR (500 MHz, $CDCl_3$): δ 8.01 (s, 1H), 7.90 (s, 1H), 6.97 (s, 2H), 6.90 (s, 1H), 6.77 (d, *J* = 2.6 Hz, 1H), 6.69 (d, *J* = 2.6 Hz, 1H), 6.66 (d, *J* = 4.0 Hz, 1H), 6.59 (s, 1H), 6.47 (d, *J* = 2.5 Hz, 1H), 6.37 (d, *J* = 4.2 Hz, 1H), 6.09 (d, *J* = 4.2 Hz, 1H), 2.73 (dd, *J* = 13.8, 7.0 Hz, 2H), 2.64 (s, 3H), 2.57 (s, 3H), 2.37 (s, 3H), 2.16 (s, 3H), 2.13 (s, 6H), 1.83 – 1.77 (m, 2H), 1.42 – 1.25 (m, 18H),1.15 – 1.11 (m, 3H), 1.07 – 1.05 (m, 3H), 0.87 (d, *J* = 4.8 Hz, 6H), 0.85 (s, 3H), 0.84 (s, 3H). ^{13}C NMR (125 MHz, $CDCl_3$): δ 156.22, 150.27, 148.78, 147.09, 144.23, 143.27, 139.10, 136.47, 131.05, 130.10, 128.64, 128.45, 127.76, 126.73, 126.59, 124.83, 123.05, 122.25, 121.00, 119.37, 118.62, 118.28, 117.16, 40.37, 39.54, 37.62, 37.60, 37.46, 32.97, 32.86, 32.08, 31.15, 29.85, 28.14, 24.96, 24.62, 23.97, 22.87, 22.78, 22.61, 21.31, 21.11, 20.20, 19.91, 19.81, 16.31, 14.76, 14.26. HRMS (ESI+) *m*/*z* calcd para $C_{56}H_{70}B_2F_4N_4O_2Na$ $[M+Na]^+$ 951.5545. Found 951.5531.

Supporting information

Potential energy curve of different torsion angles between the two BODIPY units forming the dimer **4.** Photophysical parameters and the absorption and emission spectra of compounds **5-20**. Area under the curve of the main absorption band of compounds **4** and **5** after the deconvolution in two gaussians and oscillator strength of each transition obtained

by theoretical simulations of **4**, **5**, **15** and **18**. Electron density maps of dimer **20**. ^{1}H and ^{13}C NMR spectra of the compounds prepared. cartesian coordinates and total energy.

The Supporting Information is available free of charge on the ACS Publications website at DOI: xxxxx

Author information:

Corresponding Author:

*Email: virginia.martinez@ehu.eus, eduardop@ugto.mx

ORCID

Eduardo Peña-Cabrera: 0000-0002-2069-6178

Rebeca Sola-Llano: 0000-0003-1998-3644

Iñigo López Arbeloa: 0000-0002-8440-6600

Virginia Martínez-Martínez: 0000-0001-7551-3714

Ismael J. Arroyo-Córdoba: 0000-0002-1904-9707

Author Contribution

‡These authors contributed equally.

Notes

The authors declare no competing financial interest.

Acknowledgements

Financial support from Gobierno Vasco (IT912-16), Ministerio de Economía y Competitividad "MINECO" (MAT2017-83856-C3-3-P), and CONACyT (grants 253623, 123732) is acknowledged. I. J. A.-C. thanks CONACyT for graduate scholarship. Donation of 2,6-dimethyl-8-methylthioBODIPY by Cuantico de Mexico (www.cuantico.mx) is appreciated.

References

(1) Haugland, R. P. The Handbook. A Guide to Fluorescent Probes and Labeling Technologies, 10th edn.; Molecular Probes Inc: Eugene, Oregon, USA, 2005.

(2) Ziessel, R.; Ulrich, G.; Harriman, A. *New J. Chem*. **2007**, *31*, 496–501.

(3) Ulrich, G.; Ziessel, R.; Harriman, A. *Angew. Chemie - Int. Ed*. **2008**, *47*, 1184–1201.

(4) Benniston, A. C.; Copley, G. *Phys Chem Chem Phys* **2009**, *11*, 4124–4131.

(5) Loudet, A.; Burgess, K. *Chem Rev* **2007**, *107*, 4891–4932.

(6) Wood, T. E.; Thompson, A. *Chem Rev* **2007**, *107*, 1831–1861.

(7) Lakshmi, V.; Rao, M. R.; Ravikanth, M. *Org. Biomol. Chem.* **2015**, *13*, 2501–2517.

(8) Lakshmi, V.; Sharma, R.; Ravikanth, M. *Reports Org. Chem.* **2016**, *6*, 1–24.

(9) Boens, N.; Verbelen, B.; Dehaen, W. *Eur. J. Org. Chem.* **2015**, 6577–6595.

(10) Kamkaew, A.; Lim, S. H.; Lee, H. B.; Kiew, L. V.; Chung, L. Y.; Burgess, K. *Chem. Soc. Rev.* **2013**, *42*, 77–88.

(11) Belmonte-Vázquez, J. L.; Sola-Llano, R.; Bañuelos, J.; Betancourt-Mendiola, L.; Vázquez-Guevara, M. A.; López-Arbeloa, I.; Peña-Cabrera, E. *Dye. Pigment.* **2017**, *147*, 246–259.

(12) Gómez-Durán, C. F. A.; Esnal, I.; Valois-Escamilla, I.; Urías-Benavides, A.; Bañuelos, J.; López Arbeloa, I.; García-Moreno, I.; Peña-Cabrera, E. *Chem. - A Eur. J.* **2015**, *22*, 1048–1061.

(13) Duran-Sampedro, G.; Agarrabeitia, A. R.; Garcia-Moreno, I.; Gartzia-Rivero, L.; de la Moya, S.; Bañuelos, J.; López-Arbeloa, Í.; Ortiz, M. J. *Chem. Commun.* **2015**, *51*, 11382–11385.

(14) Durán-Sampedro, G.; Epelde-Elezcano, N.; Martínez-Martínez, V.; Esnal, I.; Bañuelos, J.; García-Moreno, I.; Agarrabeitia, A. R.; de la Moya, S.; Tabero, A.; Lazaro-Carrillo, A.; Villanueva, A.; Ortiz, M. J.; López-Arbeloa, I. *Dye. Pigment.* **2017**, *142*, 77–87.

(15) Bhattacharyya, U.; Kumar, B.; Garai, A.; Bhattacharyya, A.; Kumar, A.; Banerjee, S.; Kondaiah, P.; Chakravarty, A. R. *Inorg. Chem.* **2017**, *56*, 12457–12468.

(16) Cakmak, Y.; Kolemen, S.; Duman, S.; Dede, Y.; Dolen, Y.; Kilic, B.; Kostereli, Z.; Yildirim, L. T.; Dogan, A. L.; Guc, D.; Akkaya, E. U. *Angew. Chemie - Int. Ed.* **2011**, *50*, 11937–11941.

(17) Bröring, M.; Krüger, R.; Link, S.; Kleeberg, C.; Köhler, S.; Xie, X.; Ventura, B.; Flamigni, L. *Chem. - A Eur. J.* **2008**, *14*, 2976–2983.

(18) Bruhn, T.; Pescitelli, G.; Jurinovich, S.; Schaumlöffel, A.; Witterauf, F.; Ahrens, J.; Bröring, M.; Bringmann, G. *Angew. Chem. Int. Ed.* **2014**, *53*, 14592–14595.

(19) Wang, J.; Wu, Q.; Wang, S.; Yu, C.; Li, J.; Hao, E.; Wei, Y.; Mu, X.; Jiao, L. *Org. Lett.* **2015**, *17*, 15–18.

(20) Nepomnyashchii, A. B.; Bröring, M.; Ahrens, J.; Bard, A. J. *J. Am. Chem. Soc.* **2011**, *133*, 8633–8645.

(21) Hayashi, Y.; Yamaguchi, S.; Cha, W. Y.; Kim, D.; Shinokubo, H. *Org. Lett.* **2011**, *13*, 2992.

(22) Gai, L.; Lu, H.; Zou, B.; Lai, G.; Shen, Z.; Zhifang Li. *RSC Adv.* **2012**, *2*, 8840–8846.

(23) Rihn, S.; Erdem, M.; De Nicola, A.; Retailleau, P.; Ziessel, R. *Org. Lett.* **2011**, *13*, 1916.

(24) Epelde-Elezcano, N.; Palao, E.; Manzano, H.; Prieto-Castañeda, A.; Agarrabeitia, A. R.; Tabero, A.; Villanueva, A.; de la Moya, S.; López-Arbeloa, I.; Martínez-Martínez, V.; Ortiz, M. J. *Chem. Eur. J.* **2017**, *23*, 4837–4848.

(25) Jiao, L.; Yu, C.; Li, J.; Wang, Z.; Wu, M.; Hao, E. *J. Org. Chem.* **2009**, *74*, 7525–7528.

(26) Verbelen, B.; Boodts, S.; Hofkens, J.; Boens, N.; Dehaen, W. *Angew. Chem. Int. Ed* **2015**, *54*, 4612–4616.

(27) Buyukcakir, O.; Bozdemir, O. A.; Kolemen, S.; Erbas, S.; Akkaya, E. U. *Org. Lett.* **2009**, *11*, 4644–4647.

(28) Lundrigan, T.; Thompson, A. *J. Org. Chem.* **2013**, *78*, 757–761.

(29) Stachelek, P.; Alsimaree, A. A.; Alnoman, R. B.; Harriman, A.; Knight, J. G. *J. Phys. Chem. A* **2017**, *121*, 2096–2107.

(30) Courtis, A. M.; Santos, S. A.; Guan, Y.; Hendricks, J. A.; Ghosh, B.; Szantai-Kis, D. M.; Reis, S. A.; Shah, J. V.; Mazitschek, R. *Bioconjug. Chem.* **2014**, *25*, 1043–1051.

(31) Sun, J.; Perfetti, M. T.; Santos, W. L. *J. Org. Chem.* **2011**, *76*, 3571.

(32) Chen, J.; Burghart, A.; Derecskei-Kovacs, A.; Burgess, K. *J. Org. Chem.* **2000**, *65*, 2900–2906.

(33) Wagner, R. W.; Lindsey, J. S. *Pure Appl. Chem.* **1996**, *68*, 1373–1380.

(34) Betancourt-Mendiola, L.; Valois-Escamilla, I.; Arbeloa, T.; Bañuelos, J.; López Arbeloa, I.; Flores-Rizo, J. O.; Hu, R.; Lager, E.; Fernando, C.; Gómez-Durán, A.; Belmonte-Vázquez, J. L.; Martínez-Gonzalez, M. R.; Arroyo, J.; Osorio-Martínez, C. A.; Alvarado-Martínez, E.; Urías-Benavides, A.; Gutierrez-Ramos, B. D.; Tang, B. Z.; Peña-Cabrera, E. *J. Org. Chem.* **2015**, *80*, 5771–5782.

(35) Flores-Rizo, J. O.; Esnal, I.; Osorio-Martínez, C. A.; Bañuelos, J.; López Arbeloa, I.; Pannell, K. H.; Metta-Megaña, A. J.; Peña-Cabrera, E. *J. Org. Chem.* **2013**, *78*, 5867–5877.

(36) Esnal, I.; Valois-Escamilla, I.; Gómez-Durán, C. F. A.; Urías-Benavides, A.; Betancourt-Mendiola, M. L.; Lõpez-Arbeloa, I.; Bañuelos, J.; García-Moreno, I.; Costela, A.; Peña-Cabrera, E. *ChemPhysChem* **2013**, *14*, 4134–4142.

(37) Wang, S.; Lu, H.; Wu, Y.; Xiao, X.; Li, Z.; Kira, M.; Shen, Z. *Chem. - An Asian J.* **2017**, *12*, 561–567.

(38) Dolomanov, O.V.; Bourhis, L.J.; Gildea, R.J.; Howard, J.A.K.; Puschmann, H. *J. Appl. Cryst* **2009**, *42*, 339

(39) Sheldrick, G.M. *Acta Cryst* **2008**, *A64*, 112.

(40) Sheldrick, G.M. *Acta Cryst*. **2015**, *C71*, 3.

TOC


Late
functionalization
SMe
R
Early
functionalization
Formylation.
halogenation, etc.
Exchangeable
Knoevenagel
condensation
C-H activation
SMe